Original Article

MOLECULAR METABOLISM

# Arginine deprivation/citrulline augmentation with ADI-PEG20 as novel therapy for complications in type 2 diabetes

**Ammar A. Abdelrahman[1,3], Porsche V. Sandow[1,3], Jing Wang[3,5], Zhimin Xu[2,3], Modesto Rojas[1,2,3], John S. Bomalaski[4], Tahira Lemtalsi[2,3], Ruth B. Caldwell[2,3,5], Robert W. Caldwell[1,2,3,*]**

## ABSTRACT

**Objective:** Chronic inflammation and oxidative stress mediate the pathological progression of diabetic complications, like diabetic retinopathy (DR), peripheral neuropathy (DPN) and impaired wound healing. Studies have shown that treatment with a stable form of arginase 1 that reduces L-arginine levels and increases ornithine and urea limits retinal injury and improves visual function in DR. We tested the therapeutic efficacy of PEGylated arginine deiminase (ADI-PEG20) that depletes L-arginine and elevates L-citrulline on diabetic complications in the *db/db* mouse model of type 2 diabetes (T2D).

**Methods:** Mice received intraperitoneal (IP), intramuscular (IM), or intravitreal (IVT) injections of ADI-PEG20 or PEG20 as control. Effects on body weight, fasting blood glucose levels, blood-retinal-barrier (BRB) function, visual acuity, contrast sensitivity, thermal sensitivity, and wound healing were determined. Studies using bone marrow-derived macrophages (BMDM) examined the underlying signaling pathway.

**Results:** Systemic injections of ADI-PEG20 reduced body weight and blood glucose and decreased oxidative stress and inflammation in *db/db* retinas. These changes were associated with improved BRB and visual function along with thermal sensitivity and wound healing. IVT injections of either ADI-PEG20, anti-VEGF antibody or their combination also improved BRB and visual function. ADI-PEG20 treatment also prevented LPS/IFN$_{\gamma}$-induced activation of BMDM *in vitro* as did depletion of L-arginine and elevation of L-citrulline.

**Conclusions/interpretation:** ADI-PEG20 treatment limited signs of DR and DPN and enhanced wound healing in *db/db* mice. Studies using BMDM suggest that the anti-inflammatory effects of ADI-PEG20 involve blockade of the JAK2-STAT1 signaling pathway via L-arginine depletion and L-citrulline production.



**Keywords** Diabetic complications; Arginase 1; Arginine deiminase; Visual function; Anti-inflammatory; L-arginine; L-citrulline

## 1. INTRODUCTION

Diabetes mellitus is a major health problem, affecting millions worldwide [1]. Expansion of diabetic and aging populations contributes to the high incidence of diabetic complications including diabetic retinopathy (DR), peripheral neuropathy (DPN), and impaired wound healing [1,2]. Preventive measures for diabetic complications rely largely on tight glycemic control which is challenging, with limited compliance [3]. Treatment of diabetic complications is also difficult and mainly targets late-stage complications after tissue damage has occurred [4]. Current pharmacologic therapies for DR depend largely on intravitreal injections of anti-VEGF or steroids. This approach risks retinal damage and requires expensive tools and experienced practitioners, making it largely inaccessible to underserved populations [5,6]. Thus, the search for systemic treatments of DR, which can reduce retinal inflammation, oxidative stress, and blood-retinal-barrier (BRB) dysfunction, is extremely important.

DPN is also a common complication of diabetes, especially in patients with type 2 diabetes (T2D). Current prevention strategy focuses on enhanced glycemic control to decrease episodes of hyperglycemia. However, T2D patients gain little, if any, protection with tight glycemic control [7]. Management strategies for DPN focus mainly on symptomatic treatment of neuropathic pain [8]. Disease-modifying therapies have not provided significant clinical improvement, and many trials

[1]Department of Pharmacology and Toxicology, Medical College of Georgia, Augusta University, Augusta, GA, 30912 USA [2]Vascular Biology Center, Medical College of Georgia, Augusta University, Augusta, GA 30912 USA [3]Culver Vision Discovery Institute, Medical College of Georgia, Augusta University, Augusta, GA 30912 USA [4]Polaris Pharmaceuticals, Inc., San Diego, CA 92121, USA [5]Department of Cellular Biology and Anatomy, Medical College of Georgia, Augusta University, Augusta, GA 30912 USA

*Corresponding author. Department of Pharmacology and Toxicology, Medical College of Georgia, Augusta University, Augusta, GA, USA.

E-mails: aamar@wustl.edu (A.A. Abdelrahman), wcaldwel@augusta.edu (R.W. Caldwell).

*Abbreviations:* ADI, Arginine deiminase; ASS-1, Argininosuccinate synthase; ASL-1, Argininosuccinate lyase; BMDM, Bone marrow-derived macrophage; BRB, Blood-retinal-barrier; DPN, Diabetic peripheral neuropathy; DR, Diabetic retinopathy; T2D, Type 2 diabetes; IL-1β, Interleukin 1-beta; IM, Intramuscular; iNOS, inducible Nitric oxide synthase; IP, Intraperitoneal; IVT, Intravitrea; TNF-α, Tumor necrosis factor-alpha; VEGF, Vascular endothelial growth factor

Received July 7, 2024 • Revision received August 13, 2024 • Accepted August 26, 2024 • Available online 29 August 2024

https://doi.org/10.1016/j.molmet.2024.102020

 

have shown ambiguous results [7,8]. Progression of DPN usually becomes complicated by impaired wound healing which leads to a greater risk of debilitating foot ulcers and amputations [9].
Uncontrolled inflammation, upregulated oxidative/nitrative stress, and impaired immune function are common factors in most diabetic complications, and are critically involved in the pathogenesis of DR, DPN, and impaired wound healing [10]. Previously, we have shown the potential of L-arginine depletion with a stable pegylated form of arginase 1 as a neuroprotective anti-inflammatory therapy in mouse models of DR, ischemic retinopathy and CNS ischemia [11–13]. Arginase 1 cleaves L-arginine into urea and L-ornithine [14]. Depletion of circulating L-arginine has been shown to halt the growth of certain cancers which require L-arginine for growth, and are unable to recycle L-citrulline back into L-arginine because they lack argininosuccinate synthase (ASS-1) or argininosuccinate lyase (ASL-1) [15,16].
Currently, several amino-acid depleting agents — including L-arginine depleting enzymes — are in clinical trials for cancer therapy [17–19]. Arginine deiminase (ADI) is a high affinity bacterial enzyme that catalyzes the hydrolysis of the imino group of L-arginine to produce equal molar amounts of L-citrulline, along with ammonia [15]. A PEGylated stable form of ADI (ADI-PEG20) enhances the half-life of intravenously injected ADI from 4.7 to 53 h in mice and reduces its immunogenicity [20]. Further studies have shown that the ADI-PEG20 half-life in mice is 34.5 h with intramuscular injections, and 26.7 h with subcutaneous injections [21]. This formulation of ADI can markedly deplete circulating plasma levels of L-arginine from roughly 130 μM to less than 2 μM in mice, pigs, and humans, while greatly elevating levels of L-citrulline from less than 50 μM to over 500 μM [22–24]. L-citrulline has anti-inflammatory properties, and has been shown to limit oxidative stress and improve mitochondrial biogenesis in the cardiovascular system, skeletal muscle, and central nervous system [23,25–28]. ADI-PEG20 recently demonstrated improved overall survival in a phase 3 clinical trial in pleural mesothelioma [29].
Here, we examined the effectiveness of ADI-PEG20 in protecting against DR, DPN and impaired wound healing in a mouse model of T2D. We used the leptin receptor deficient *db/db* mouse model which exhibits impaired retinal functions, disrupted peripheral sensory function, and delayed wound healing [30–32]. We evaluated the potential of systemic delivery of ADI-PEG20 to correct these pathological processes, and further tested the effectiveness of intravitreal ADI-PEG20 delivery to protect retinal functions in the *db/db* mouse. Studies in BMDMs examined potential mechanisms of the ADI-PEG20 anti-inflammatory actions.

## 2. MATERIALS AND METHODS

### 2.1. Animal model

Studies were performed following the Association for Research in Vision and Ophthalmology (ARVO) Statement for the use of animals in ophthalmic and vision research and were approved by the Augusta University Institutional Animal Care and Use Committee. Mice were maintained at ambient temperature on a 12:12 h light/dark cycle and fed ad libitum. Male *db/db* male mice (B6·BKS(D)-*Lepr*$^{db}$/J - Stock No. 000697) and their male Db/+ littermates were obtained from Jackson Laboratories (Bar Harbor, ME). Mice were housed in standard shoebox cages (n = 5/cage) with continuous access to water and standard chow (Teklad 8904). Groups of *db/db* mice (16 weeks, when blood glucose increase reaches plateau) were treated twice weekly with either intraperitoneal (IP) or intramuscular (IM) injections of ADI-PEG20 (0.1 IU/gm). Twice weekly injections were given based on reports that the half-life of ADI-PEG20 in mice which is 34.5 h with intramuscular injections and 26.7 h with subcutaneous injections [21]. Pharmaceutical grade ADI-PEG20 was provided by Polaris Pharmaceuticals, Inc (San Diego, CA). ADI-PEG20 is a recombinant arginine deiminase covalently linked to PEG of 20,000 MW which increases its half-life to about 10 days and decreases its immunogenicity [20]. PEG 20 (0.1 IU/gm PEG 20,000 MW) dissolved in histidine and 130 mM NaCl buffer, (pH 6.6 to 7.0) was used as vehicle control.
Mice were assigned randomly to drug or vehicle control groups. All analyses were performed by investigators blinded to the treatments. The IP treatments were continued for 4 weeks and the IM injections were continued for 12 weeks. Body weight was measured before each injection to ensure appropriate dosing and to monitor weight change. During the 12-week study, blood glucose levels from tail tip samples were measured using a glucometer at 0, 4, 8, and 12 weeks after the start of treatment. In both studies, mice were sacrificed 3 days after the last dose, and their eyes were collected and prepared for analysis. For intravitreal (IVT) injection, one eye of each mouse received drug while the other received vehicle. Mice were treated at 16 weeks and tested 7 and 14 days later. Each eye received 1 μl of goat anti-mouse VEGF164 (AF-493-NA; R&D Systems, 200 ng), ADI-PEG20 (34 ng), combination, or vehicle (PEG20). Dose of ADI-PEG20 was based on equivalent enzyme activity compared to our previously published trials with PEG-Arginase1 [33]. Sterile filtered phosphate-buffered saline (PBS) was used to prepare the proper dilution. Lean littermate Db/+ mice received 1 μl of PBS to control for injection effects.

### 2.2. Visual function studies

Visual acuity and contrast sensitivity were assessed using optokinetic response tracking (OKT) (Cerebral Mechanics, Inc., Lethbridge, AB, Canada) as described with minor modifications [34]. Briefly, sine wave gratings were displayed across four LCD screens revolving around a central stand. The optomotor reflex of the unrestrained mouse to the rotating vertical sine wave grating was recorded by manual tracking of reflexive head movements. To determine spatial frequency thresholds for visual acuity, an increasing stairstep algorithm was utilized starting at 0.042 cycles/deg (c/d) with 100% contrast. To determine the contrast threshold, the spatial frequency was fixed at 0.092 c/d and a decreasing stairstep algorithm was utilized starting with the maximum contrast [35]. Manual tracking of visual reflexes was performed by an investigator blinded to treatment status. Readings from clockwise (left eye) or counterclockwise (right eye) were recorded and the average for each mouse was used in the data analysis for mice treated with IP and IM injections. For IVT injections, one eye received the indicated treatment diluted in PBS and the other eye received PBS as vehicle control. For mice treated systemically, data from both eyes of one mouse was averaged in statistical analysis.

### 2.3. Thermal sensitivity test for peripheral neuropathy

To assess diabetic neuropathy, we monitored hind limb withdrawal to elevated temperature. For the 4-week study, mice were placed on a heated plate at 42°C in a room with controlled temperature (25 °C). The plate temperature was then increased at 3°C/min. Response time and temperature were recorded by the software (HotScan, AccuScan Instruments, Inc. Columbus, OH). For the 12-week study, hind limb withdrawal time from a static 50 °C-plate was visually detected and recorded with the press of foot petal (HOT Plate Analgesia Meter, IITC INC. Woodland Hills, CA). Mice were immediately removed once the response was detected to avoid injury.

### 2.4. Wound healing assay

Groups of *db/db* mice (16 week old) received ADI-PEG20 or PEG20 (0.1 IU/gm, IP) twice weekly for three weeks. Mice were anesthetized using

 

isoflurane and the dorsal skin was shaved and cleaned with povidone-iodine solution followed by 70% alcohol. One circular, full-thickness dorsal skin wound was created on each mouse using a 6 mm biopsy punch. A single dose of extended-release buprenorphine (Ethiqa XR, Fidelis Pharmaceuticals, North Brunswick, NJ) was administered for analgesia. Mice were placed on a warming pad (37 °C) until fully recovered from anesthesia. Images of the wounds were taken immediately after wounding and every two days for 8 days with a standard metric ruler placed adjacent to the wounds. Wound areas were determined using ImageJ software. The degree of wound closure was calculated as a percentage of the baseline wound area.

### 2.5. Tissue collection and immunofluorescence imaging

Mice were anesthetized via isoflurane inhalation and perfused through the left ventricle with phosphate buffer saline (PBS, 5 min). One retina from each mouse was prepared for western blot analysis and the other whole eye was fixed in 4% paraformaldehyde and prepared for cryosection sectioning for immunofluorescence studies [34]. The following primary antibodies were used: 3-nitrotyrosine (3-NT) (Sigma—Aldrich Cat. #N0409, St. Louis, MO, USA; 1:300) and 4-hydroxynonenal (4-HNE) (Abcam Cat. # ab46545, Cambridge, MA, USA; 1:50). Imaging was performed using a Carl Zeiss 780 multiphoton confocal microscope.

### 2.6. Blood-retinal-barrier (BRB) function

Disruption of BRB and vascular leakage were assessed by measurement of albumin extravasation as previously described [13]. The amount of tissue albumin in the retina protein lysate after trans-cardiac perfusion was quantified by western blot.

### 2.7. Western blot analysis

Retina protein lysates were separated on sodium dodecyl sulfate (SDS)-polyacrylamide gels, transferred to polyvinylidene fluoride (PVDF), blocked in 3% BSA (Bio-Rad, Hercules, CA, USA), and then incubated overnight at 4 °C with the following antibodies prepared in 3% BSA: tubulin (Sigma—Aldrich Cat. # T-9026, St. Louis, MO, USA; 1:1000), albumin (Proteintech Cat. # 16475-1-AP, Rosemont, IL, USA; 1:1000), TNFα (Abcam, Cat. # ab1793, Cambridge, MA, USA, 1:1000), iNOS (Santa Cruz Biotech. Cat # sc-7271, Dallas, Texas, USA; 1:500) and IL-1β (Bioss Cat # BS-0812R, Woburn, Massachusetts, USA; 1:500). The next day, membranes were washed three times in Tris-buffered saline with 0.5% Tween-20 (TBS-T), and then incubated with the corresponding horseradish peroxidase-conjugated secondary antibody (GE Healthcare, Piscataway, NJ, USA; 1:1000) for 1 h at room temperature. Signals were detected using an enhanced chemiluminescence system (GE Healthcare Bio-Science Corp., Piscataway, NJ, USA) and quantified by densitometry using ImageJ software (version 1.49, National Institutes of Health, Bethesda, MD, USA) and normalized to the loading control.

### 2.8. Spectral domain OCT analysis of retinal structure

Mice were anesthetized with 73 mg/kg ketamine hydrochloride/7.3 mg/kg xylazine hydrochloride (Sigma—Aldrich Co, St. Louis, MO). Pupils were dilated with 1% tropicamide (Bausch & Lomb, Tampa, FL, USA), followed by application of GenTeal Lubricant Eye Gel (Alcon, Fort Worth, TX, USA), and Systane lubricant eye drops (Alcon). The Bioptigen Spectral Domain Ophthalmic Imaging System, SDOIS (Bioptigen Envisu R2200, Morrisville, NC, USA) was used as described previously [36].

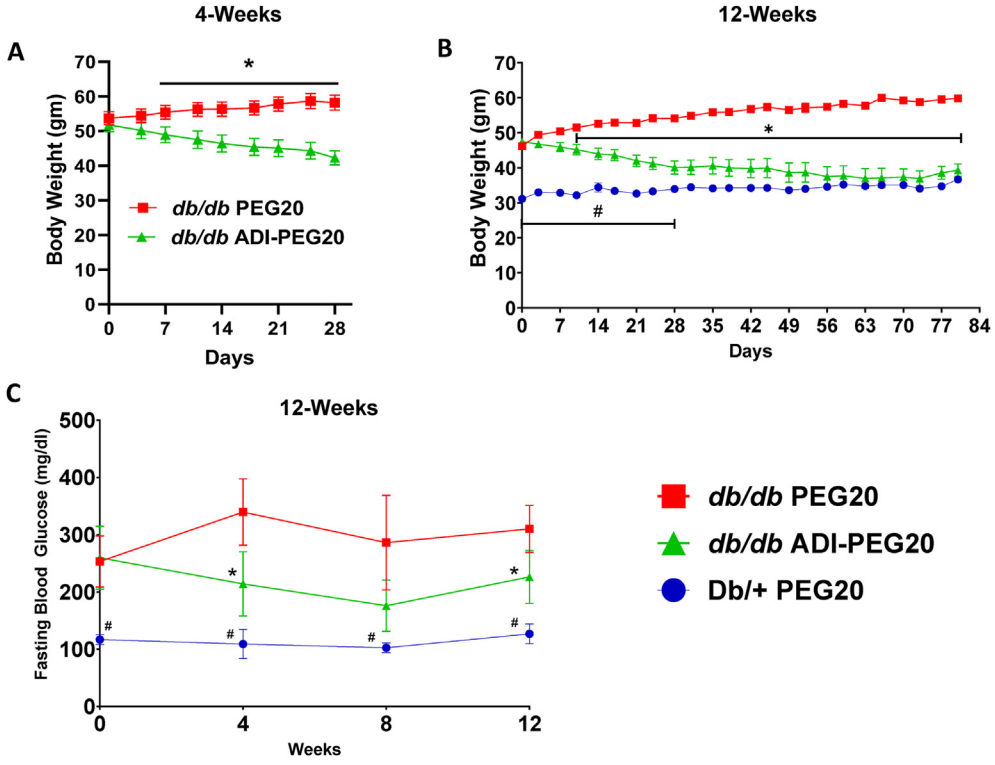


**Figure 1: Systemic ADI-PEG20 treatment decreases body weight and lowers fasting blood glucose. (A)** Body weights of *db/db* mice treated twice weekly with IP injections of ADI-PEG20 or PEG20 over the course of the 4-week study ($n = 10–11$/group). **(B)** Body weights of *db/db* mice and lean Db/+ mice treated by IM injection during the 12-week study ($n = 9–10$/group). **(C)** Fasting blood glucose levels measured during the 12-week study ($n = 5–10$/group). $^{*}p < 0.05$ for *db/db* ADI-PEG20 vs *db/db* PEG20, $^{\#}p < 0.05$ for Db/+ PEG20 vs *db/db* ADI-PEG20.

 

Thickness of the retinal layers was generated using DIVERS software included with the instrument.

### 2.9. Plasma levels of L-citrulline

Blood was collected from the tail vein (4, 8, and 12 weeks) and centrifuged at 1500 rpm for 15 min 4 °C to separate plasma from red blood cells. Plasma was sent to Polaris Pharmaceuticals for HPLC analysis of L-citrulline levels [37].

### 2.10. Bone marrow-derived macrophage (BMDM) isolation and preparation

C57BL/6J mice (8–12 week) were sacrificed and hindlegs were dissected. Using aseptic techniques, bone marrow was extracted from tibia and femur bones following removal of surrounding muscles and soft tissue. Joints were cut, and the exposed bone marrow was flushed out with RPMI 1640 medium using a 5 ml syringe and a 25-gauge needle. The cell suspension was centrifuged (1500 rpm, 10 min). Cells were seeded in a 12 well plate and induced to differentiate by treatment with M-CSF (10 ng/ml) in RMPI-1640 medium (R8758, Sigma–Aldrich Co.) with 10% FBS for 7 days. Media was changed 4 days post cell isolation. Before treatment, BMDMs were serum deprived for at least 4 h. Then interferon gamma (IFNγ, 10 ng/ml) was added to serum free RMPI1640 medium (R8758) and incubation was continued overnight. Cells were exposed to IFNγ (10 ng/ml) + lipopolysaccharide (LPS) (100 ng/ml) with graded concentrations of ADI-PEG20 or control PEG20 for 24 h. Homogenates were then collected for western blot analysis of iNOS, TNF-α and IL-1β.

For L-arginine and L-citrulline treatment, modified RPMI-1640 was used (R1780, Sigma–Aldrich) without L-arginine, L-leucine, L-lysine and phenol red. Before use, L-leucine (50 mg/L) and L-lysine (40 mg/L) were added to the medium. BMDMs were first serum starved and then treated with IFNγ overnight as stated before. Cells were treated with IFNγ + LPS in either modified RPMI-1640 medium containing 120 μM L-arginine (normal plasma levels), 2 μM L-arginine (plasma levels observed with ADI-PEG20 treatment), 50 μM L-citrulline (normal plasma levels), or. 500 μM, L-citrulline (plasma levels observed with ADI-PEG20 treatment). After 24 h, cell lysates were collected for western blot analysis.

### 2.11. Statistical analysis

Data are presented as mean ± SEM. Outlying data points >3 standard deviations from the mean were removed from calculations. Statistical analyses were performed using ANOVA with a Tukey post-test. Values $p < 0.05$ were considered statistically significant. For paired results obtained from right and left eye from the same mouse, mixed effects analysis was used followed by two-stage linear step-up procedure of Benjamini, Krieger and Yekutieli for multiple comparisons [38]. These analyses were performed using GraphPad Prism, version 9.4.1 (GraphPAD Software Inc.).

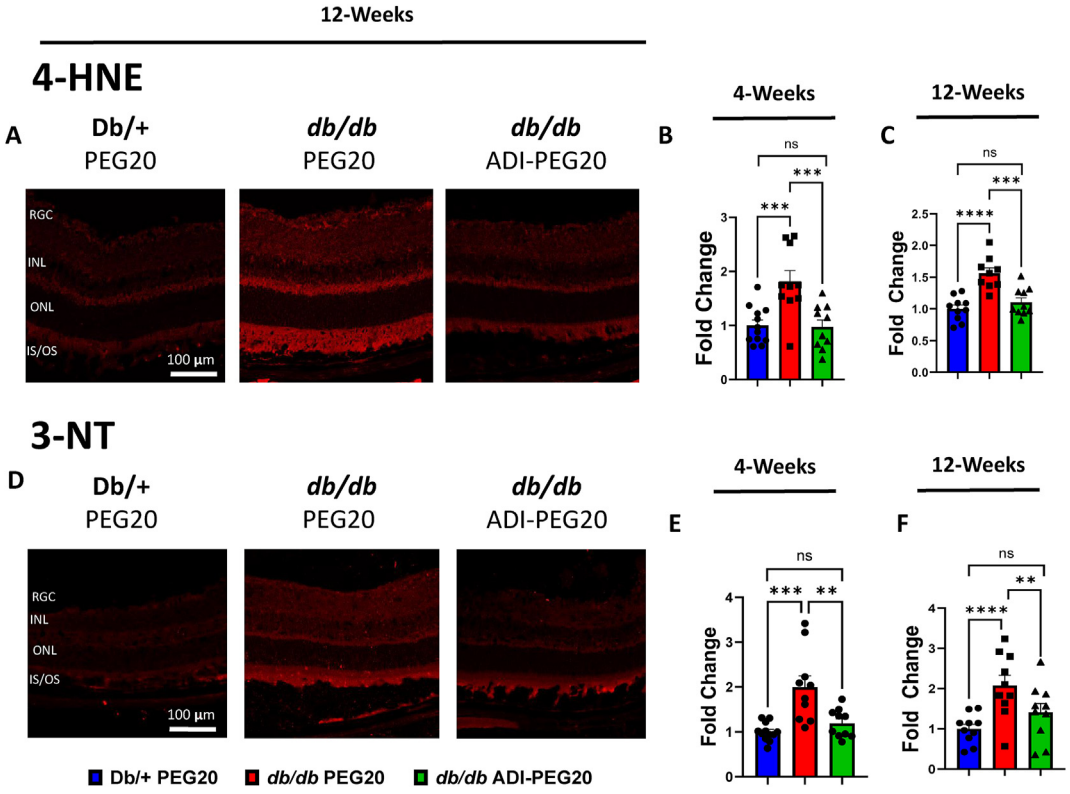


**Figure 2: ADI-PEG20 treatment reduces oxidative and nitrative stress in *db/db* retinas. (A)** Representative immunofluorescence images of retina sections for oxidative stress marker 4-HNE (4-hydroxynonenal) at 12-weeks and quantification of intensity in the treatment groups after 4 **(B)** and 12 **(C)** weeks ($n = 9$–10/group). **(D)** Representative immunofluorescence images of retina sections for nitrative stress marker 3-NT (3-nitrotyrosine) at 12-weeks and quantification of intensity in retinas of the treatment groups after 4 **(E)** and 12 **(F)** weeks ($n = 9$–10/group). (RGC: retinal ganglion cell layer, INL: inner nuclear layer, ONL: outer nuclear layer, IS/OS: inner/outer segment of photoreceptor) $^{**}p < 0.01$, $^{***}p < 0.001$, $^{****}p < 0.0001$.

 

## 3. RESULTS

### 3.1. ADI-PEG20 treament promotes weight loss, reduces fasting blood glucose, and increases plasma L-citrulline

During the 4-week IP treatment, ADI-PEG20 db/db mice progressively lost weight, whereas the PEG20 mice tended to gain weight (Figure 1 A) which is congruent with the reported beneficial effect of ADI-PEG20 on energy metabolism in *db/db* mice [39]. A similar pattern of weight change occurred with the 12 week IM injection study (Figure 1 B). The PEG20 *db/db* group gained weight while the ADI-PEG20 group lost weight and then plateaued, confirming a continued beneficial effect with prolonged treatment. By day 28, there was no significant difference between the ADI-PEG20 *db/db* mice and the lean, non-diabetic Db/+ mice. Over the 12-week treatment course, fasting blood glucose levels for control PEG20 *db/db* mice were higher than the ADI-PEG20 *db/db* and Db/+ mice. Fasting blood glucose in the ADI-PEG20 *db/db* mice was reduced compared with the PEG20 *db/db* control mice but remained higher than the Db/+ mice (Figure 1C). Similar to other studies [39], ADI-PEG20 injections IM elevated plasma L-citrulline levels in *db/db* mice at 4, 8 and 12 weeks, ranging between ~1000 and 650 μM, while normal levels in mice are about 60 μM [27] (Supplemental Fig. 1).

### 3.2. ADI-PEG20 treatment suppresses retinal oxidative and nitrative stress

One major driving factor of diabetic complications, including DR, is elevated retinal oxidative and nitrative stress [40]. To evaluate the effects of systemic ADI-PEG20 treatment on retinal oxidative and nitrative stress, we measured immunoreactivity to 4-hydroxynonenal (4-HNE) and 3-nitrotyrosine (3-NT), respectively, in frozen retinal sections. At the end of both the 4- and 12-weeks studies, the intensity of 4-HNE immunofluorescence, which reflects lipid peroxidation and reactive oxygen species levels, was significantly increased in retinas of vehicle PEG20-treated *db/db* mice compared with lean, non-diabetic Db/+ mice (Figure 2 A, B and C). Treatment of *db/db* mice with ADI-PEG20 prevented this alteration in both the 4- and 12-weeks studies. Additionally, 3-NT immunofluorescence intensity, a marker of peroxynitrite production and protein nitration, was significantly higher in vehicle PEG20-treated *db/db* mice compared to Db/+ mice (Figure 2 D, E and F). Treatment with ADI-PEG20 also prevented this effect.

### 3.3. ADI-PEG20 treatment reduces retinal inflammation

The role of inflammation in promoting diabetic retinal damage has been confirmed in both humans and animal models [41]. To assess the ability of ADI-PEG20 to limit pro-inflammatory processes, we measured retinal levels of the pro-inflammatory cytokines tumor necrosis factor-alpha (TNF-α) and interleukin I-beta (IL-1β) by western blot. Retinas of PEG20 vehicle-treated control mice showed elevated levels of TNF-α compared to lean Db/+ non-diabetic mice at the end of the 4-weeks and 12-weeks studies (Figure 3 A, B). IL-1β was significantly elevated in the 12-week group (Figure 3C, D). Treatment of *db/db* mice with ADI-PEG20 IP for 4-weeks and IM for 12-weeks prevented elevation of TNF-α, and blocked the rise in IL-1β at 12-weeks. Production of cytotoxic levels of nitric oxide by the inducible isoform of nitric oxide synthase (iNOS) is a well known mediator of

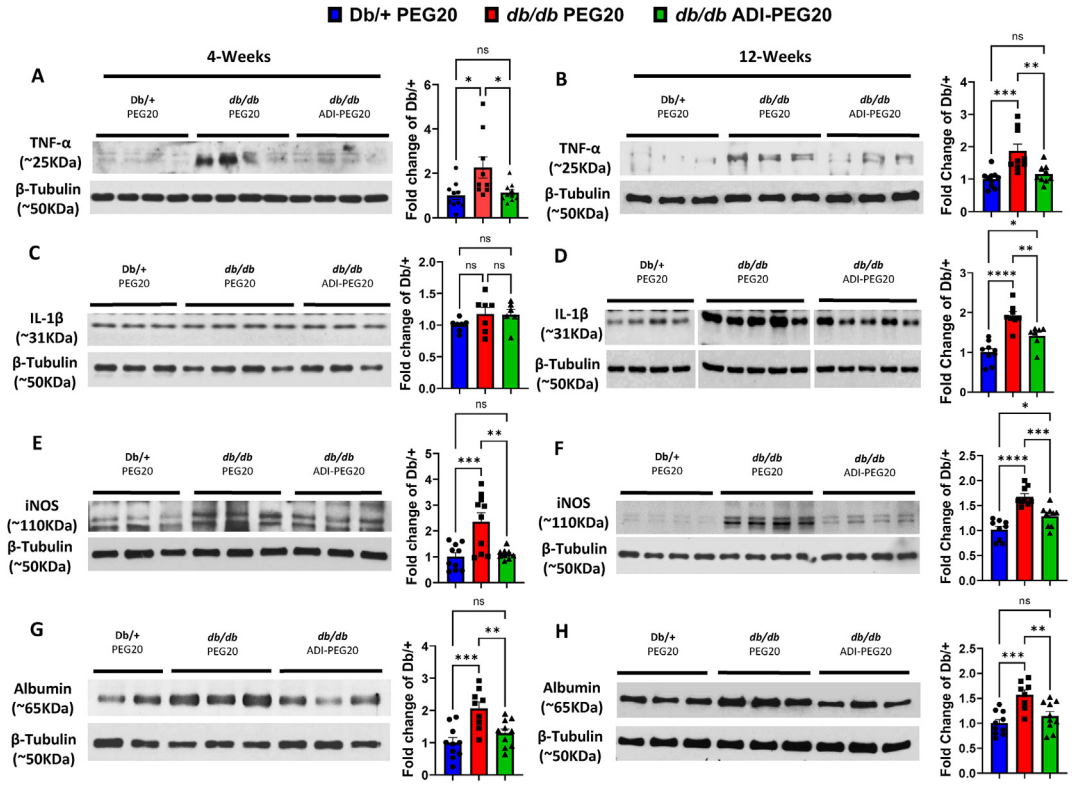


**Figure 3: ADI-PEG20 treatment reduces retinal inflammation and improves blood-retinal barrier function in *db/db* retinas.** Representative western blot and quantitation of TNF-α **(A, B)**, IL-1β **(C, D)**, and iNOS **(E, F)** in retina protein lysate after 4 and 12 weeks of treatment ($n = 6–10$/group). Representative western blots and quantitation of extravasated albumin **(G, H)** in retina protein lysate after 4 and 12 weeks of treatment ($n = 8–10$/group). ns = not significant, $*p < 0.05$, $**p < 0.01$, $***p < 0.005$, $****p < 0.0001$.

 

inflammatory damage in murine models of diabetes [42]. Levels of iNOS expression were significantly elevated in PEG20 vehicle treated *db/db* retina protein lysates compared to the lean Db/+ mice at both 4 and 12 weeks (Figure 3 E, F). Systemic IP or IM treatment with ADI-PEG20 significantly blocked these increases.

### 3.4. ADI-PEG20 treatment protects the blood–retina-barrier (BRB)

Extravasation of albumin into the retinal tissue reflects a breakdown of the BRB [43]. Retinas of *db/db* vehicle control mice showed elevated levels of albumin at both 4- and 12-weeks compared to lean Db/+ control mice (Figure 3 G, H). Treatment with ADI-PEG20 prevented this increase in both groups.

Since current drug therapies for DR are largely through intravitreal (IVT) injections of anti-VEGF or steroid drug formulations [44], we also investigated the effectiveness of IVT ADI-PEG20 compared to anti-VEGF, alone and in combination. IVT injection with ADI-PEG20 (34 ng/1 μl) significantly reduced retinal albumin level at 14 days as compared with the vehicle controls (Figure 4 A, B). Similarly, in eyes injected IVT with anti-VEGF antibody (200 ng/1 μl), retinal albumin levels were significantly lower than in eyes given vehicle injections and similar the Db/+ mice. When ADI-PEG20 was combined with anti-VEGF for IVT treatment, the albumin level was also lower and similar to the other treatment groups.

### 3.5. Intravitreal and systemic ADI-PEG20 treatment improves visual functions

We used OKT to assess visual functions in mice treated with IVT injections of ADI-PEG20. Visual acuity and contrast sensitivity at both 7- and 14-days post-injection were improved in all treatment groups (Figure 4C, D, E, F). Although the anti-VEGF treatment and the combined anti-VEGF and ADI-PEG20 treatment showed only a trend towards improvement in contrast sensitivity at 7 days post injection, contrast sensitivity was significantly improved in both groups by day 14 (Figure 4 E, F).

The effectiveness of systemic IP and IM treatments with ADI-PEG20 for 4-weeks and 12-weeks, respectively, was also examined. In the 4-week study, PEG20 vehicle *db/db* mice showed significantly lower visual acuity compared to Db/+ lean control mice. After two weeks of IP treatment with ADI-PEG20, visual acuity of the *db/db* mice was significantly improved compared to PEG20-treated *db/db* mice (Figure 5 A). However, this improvement was not maintained after four weeks of ADI-PEG20 treatment (Figure 5 A). During the IM study, visual acuity of the ADI-PEG20 db/db mice was significantly improved at four weeks and after the 12 week treatment period compared to PEG20 vehicle controls (Figure 5C). We also assessed visual contrast sensitivity function in these same mice, which was also impaired compared to Db/+ mice. In both the IP and IM study, ADI-PEG20 produced a significant improvement (lower contrast threshold) over the entire treatment periods compared to PEG20 vehicle controls (Figure 5 B, D). While effects of systemic treatment can be attributed to systemic and/or local effects, the IVT study shows that ADI-PEG20 is also effective through local mechanisms.

Spectral domain-optical cohesion tomography (SD-OCT) was utilized to measure retinal structure before and after the 4-week treatment. No difference in total retinal thickness (Supplementary Fig. 2) or thickness of the individual layers was detected among the groups (data not shown).

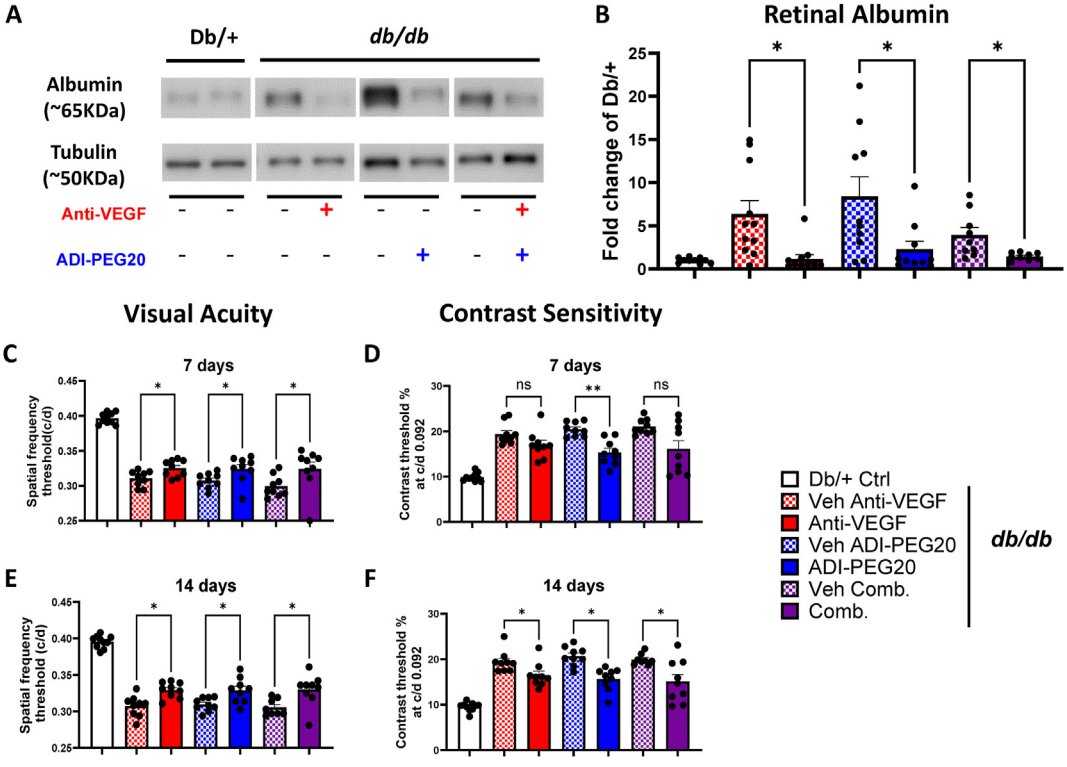


**Figure 4: Intravitreal (IVT) delivery of ADI-PEG20 and/or Anti-VEGF improves blood-retinal barrier function and visual function in *db/db* mice.** Representative western blots and quantitation of extravasated albumin **(A, B)** in retinas from mice injected IVT with ADI-PEG20, Anti-VEGF, their combination (Comb) or vehicle (PBS). Quantification is expressed as fold change from Db/+ controls ($n = 9–10$/group). Visual acuity and contrast threshold **(C–F)** for mice that received IVT treatment with anti-VEGF, ADI-PEG20, or their combination (Comb.) in one eye and PBS vehicle control in the other 7 **(C, D)** and 14 **(E, F)** days after IVT injections ($n = 9–10$/group). $^{*}p < 0.05$, $^{**}p < 0.01$.

 

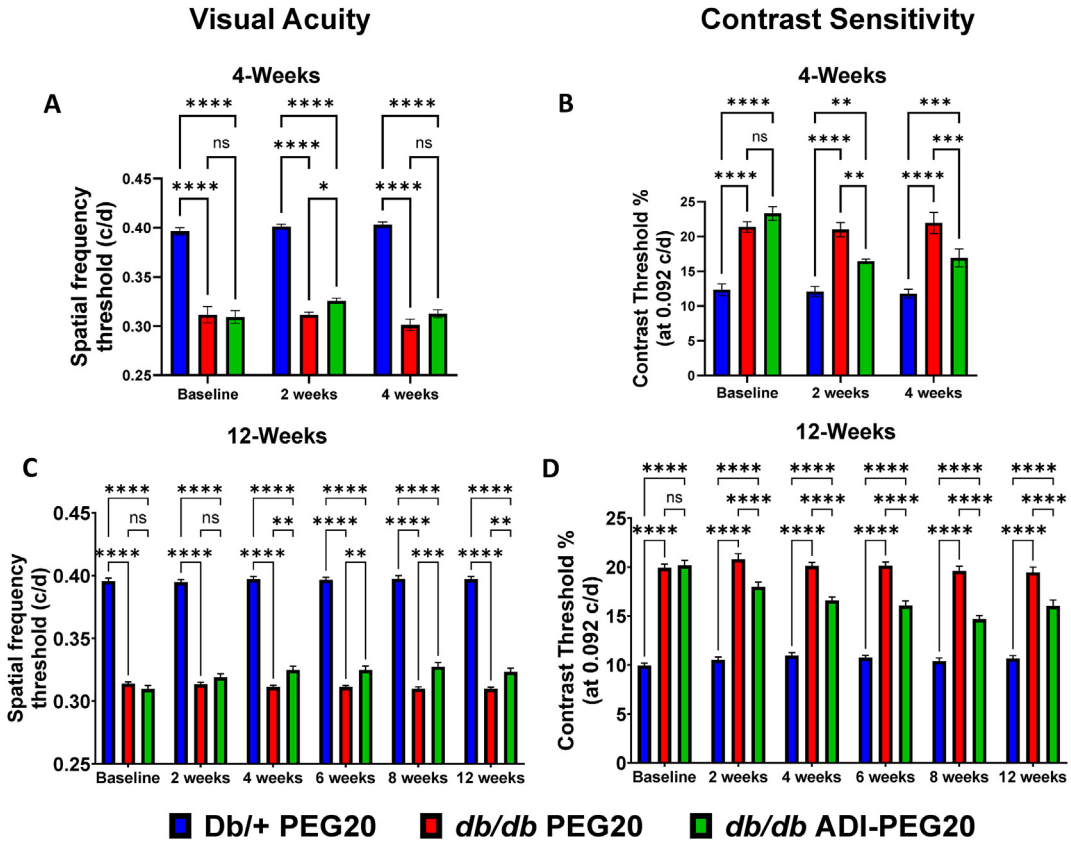


**Figure 5: Systemic ADI-PEG20 treatment improves visual functions in *db/db* mice.** Visual acuity **(A, C)**, measured as spatial frequency threshold, was determined every two weeks in the intraperitoneal (IP) 4-week and intramuscular (IM) 12-week studies (n = 9–10/group for both). Contrast sensitivity **(B, D)**, measured as contrast threshold, was also determined every two weeks in the 4- and 12-week studies (n = 9–10/group for both). ns = not significant, $^{*}p < 0.05$, $^{**}p < 0.01$, $^{***}p < 0.001$, $^{****}p < 0.0001$.

### 3.6. ADI-PEG20 treatment preserves thermal sensitivity

Peripheral sensory neuropathy is a common complication of diabetes that is also evident in the *db/db* mouse model [45]. We examined the effect of the diabetic state and ADI-PEG20 on the hind limb withdrawal response. Response times were significantly higher in PEG20 vehicle control *db/db* mice compared to lean Db/+ controls in the 4-week IP study (Figure 6 A). The ADI-PEG20 treatment prevented this impairment of thermal sensitivity in *db/db* mice throughout the 12-week IM study when mice were tested after 3, 6, 9, and 12 weeks of treatment. (Figure 6 B).

### 3.7. ADI-PEG20 treatment improves wound healing

Impaired cutaneous wound healing is another complication of diabetes [9]. We assessed the degree to which dorsal skin wounds closed over a period of 8 days (Figure 6C) after 3 weeks of IP treatments. Wound closure in the lean control Db/+ mice was the most rapid while that in the *db/db* mice treated with the PEG20 vehicle was the slowest and least complete. ADI-PEG20 treatment significantly increased the rate and degree of closure above that of the vehicle control *db/db* mice at days 6 and 8 (Figure 6 D). Together, these data confirm a systemic improvement of diabetic complications (DR, DPN, wound healing) with systemic ADI-PEG20 treatment.

### 3.8. ADI-PEG20, L-arginine, and L-citrulline effects on activated bone marrow derived macrophage (BMDM)

Our studies showed that 24 h exposure to INFγ/LPS elevated iNOS, IL-1β, and TNF-α protein levels in PEG20 control (100 ng/ml) treated BMDM (Figure 7A, B and C). The largest increase was for iNOS. Concurrent treatment with ADI-PEG20 (10, 35, or 100 ng/ml) reduced production of all three inflammatory mediators in a concentration-dependent manner.

We also examined the effects of altering levels of L-arginine and L-citrulline concentrations on iNOS, IL-1β, and TNF-α protein expression in response to INFγ/LPS. L-arginine treatment at normal *in vivo* plasma level (120 μM) allowed a robust increase in all three proteins. However, low levels of L-arginine (2 μM), a plasma level also found in animals and humans treated with ADI-PEG20 [23], completely blocked this increase (Figure 8 A, B). We also determined the effects of elevated and normal plasma levels of L-citrulline (500 and ~50 μM, respectively) that have been reported in the plasma of animals and humans treated with or without ADI-PEG20 [23]. The 500 μM L-citrulline strongly suppressed all three inflammatory mediators (Figure 8C, D). We also examined potential underlying signaling mechanisms by determining L-citrulline effects on activation/phosphorylation of JAK2 in BMDMs by assessing the ratio of p-JAK2/JAK2. As shown in Figure 8 E and F, L-citrulline (500 μM) prevented the increase in the p-JAK2/JAK2 ratio below levels to observed with INFγ/LPS treatment with normal physiological levels of L-citrulline (50 μM).

## 4. DISCUSSION

Our study examined the effects of systemically administered ADI-PEG20 on diabetes-induced visual dysfunction, retinal oxidative/nitrative stress and inflammation, and breakdown of the BRB along

 

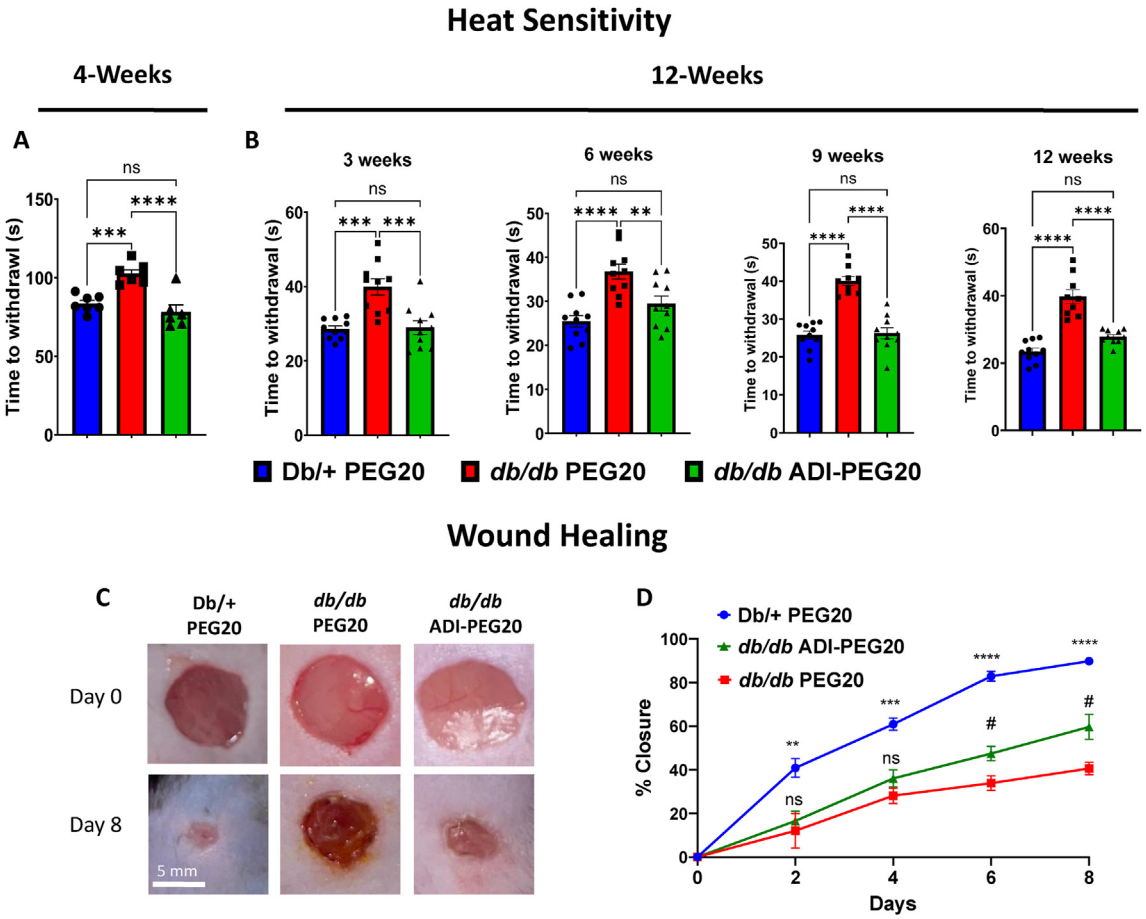


**Figure 6: Treatment with ADI-PEG20 improves heat sensitivity and wound closure.** Paw withdrawal response time to a thermal stimulus was assessed at the end of the 4-week study **(A)** and every three weeks for the 12-week study **(B)** ($n = 6–7$/group for 4-week study, $n = 9–10$/group for 12-week study). ns = not significant, $^{**}p < 0.01$, $^{***}p < 0.001$, $^{****}p < 0.0001$ Wound healing was assessed after 3 weeks of IP treatment. Representative images and quantitation **(C, D)** of wound closure progress as percentage of baseline wound area at baseline and over 8 days of treatments. ($n = 5–8$/group). ns = not significant, $\#p < 0.05$ db/db PEG20 vs *db/db* ADI-PEG20, $^{**}p < 0.01$, $^{***}p < 0.001$ and $^{***}p < 0.0001$ Db/+PEG20 vs *db/db* PEG20.

with and peripheral sensory loss, and impaired wound healing in the *db/db* mouse model of T2D. Effects of IVT injections of ADI-PEG20 alone and in combination with Anti-VEGF on BRB and visual function were also determined.

ADI is a bacterial enzyme that enables bacteria to survive in various phagocytes, and contributes to bacteria pathogenesis by protecting bacteria from acidic environments through the production of ammonia from L-arginine [46,47]. This protective mechanism may involve prevention of phagosome/lysosomal acidification and fusion and/or depletion of the L-arginine required for iNOS-induced production of bactericidal NO [15].

In a mouse model of inflammatory bowel disease, ADI-PEG20 has shown anti-inflammatory and protective effects through reduction of macrophage infiltration, and decreased iNOS expression [48]. A systemic decrease in NO production with ADI-PEG20 treatment has been shown in patients with hepatocellular carcinoma and hepatitis C virus [49]. Our study showed that systemic ADI-PEG20 treatment decreased iNOS protein in retinal lysates of obese diabetic *db/db* mice. Although the mechanisms involved are not clear, L-arginine depletion can reduce iNOS expression through phosphorylation of the mRNA translation eukaryotic initiation factor 2 $\alpha$ (eIF2$\alpha$) by the amino acid sensing protein kinase general control nonderepressible-2 (GCN2) [50]. Moreover, L-arginine depletion can inhibit mammalian target of rapamycin complex 1 (mTORC1) activation and promote autophagy, which, depending on the cellular context, can be cytoprotective or induce apoptosis [51–53]. In T2D, mTORC1 hyperactivity contributes to insulin resistance and hyper-inflammatory states associated with diabetic complications [54–56]. Suppression of mTORC1 is associated with protective anti-inflammatory responses in diabetic complications [56].

In addition to L-arginine depletion, ADI-PEG20 treatment leads to elevated L-citrulline production in both plasma and tissues including brain [23]. L-citrulline appears to be an anti-inflammatory signal that prevents pro-inflammatory macrophage activation, and reduces anti-bacterial host defense by suppressing JAK2-STAT1 signaling [57]. Evidence for this is a rapid decline in macrophage L-citrulline levels with LPS/INF-$\gamma$ stimulation and strong suppression of NO production by iNOS with supplemental L-citrulline [57]. In addition, elevated plasma L-citrulline levels due to ADI-induced conversion of L-arginine, have other favorable effects. L-citrulline can be rapidly transported into a variety of cells through L-type amino acid transporter 1, and recycled back into L-arginine by ASS-1 and ASL-1, which are expressed in most cell types [27]. Thus, normal cellular functions can be maintained. This is very important for regulation of vascular blood flow through the production of moderate levels of NO by endothelial cell NOS (eNOS) and also limits NO production by iNOS in macrophages responding to

 

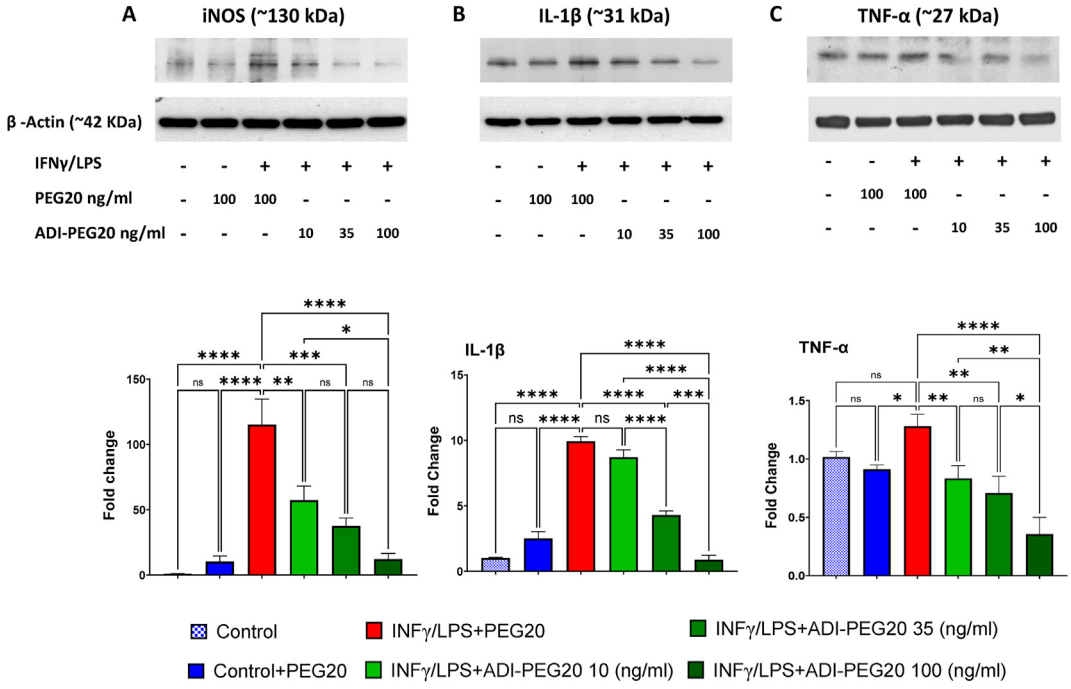


**Figure 7: Treatment with ADI-PEG20 reduces production of inflammatory markers in activated bone marrow-derived macrophages (BMDM).** Representative western blots and quantitation of iNOS **(A)**, TNF-α **(B)**, and IL-1β **(C)**, in IFNγ/LPS activated bone marrow derived macrophages (BMDM) treated with 10, 35 or 100 ng/ml of ADI-PEG20 or 100 ng/ml PEG20 as control. n = 3/group, ns = not significant, $*p < 0.05$, $**p < 0.01$, $***p < 0.001$ and $****p < 0.0001$.

inflammatory signals such as endotoxins [23,27]. The divergent ability of L-citrulline recycling to replenish L-arginine to eNOS, but not iNOS has been reported in several *in vitro* studies. This difference probably reflects the limits on L-citrulline entry and recycling in macrophages which thereby limits L-arginine availability to iNOS [27,58]. Additionally, L-citrulline can be converted to L-arginine by ASS/ASL in T-cells, thus replenishing L-arginine levels and boosting host immunity [59]. Supplemental L-citrulline has also been shown to be a therapeutic adjunct in disease states associated with L-arginine deficiencies [60]. While effects of ADI-PEG20 treatment on specific pathological complications of diabetes can be the result of tissue specific effects, generalized systemic effects cannot be excluded. A recent study reported that reduction of hepatic and systemic L-arginine levels by ADI-PEG20 increased basal caloric expenditure, improved insulin sensitivity, and reversed dyslipidemia and inflammation in obese, diabetic db/db mice [39]. This occurred through activation of systemic autophagic flux and hepatic secretion of FGF21, a factor that mimics fasting [39]. In our study, systemic ADI-PEG20 treatments resulted in progressive weight loss in the db/db mice that approached baseline Db/+ controls, and lowered fasted blood-glucose levels compared to PEG20 db/db mice at the end of the 12-week IM treatment period.

We assessed the potential efficacy of localized delivery of ADI-PEG20 by performing IVT injections. This protected against visual dysfunction, and inhibited breakdown of the BRB like the effects observed in the systemic studies. Although we did not detect an added benefit of combining ADI-PEG20 with anti-VEGF IVT injections, further evaluation of possible benefits in decreasing required doses and/or increasing dosing intervals of anti-VEGF therapy is warranted.

Systemic IP injections of ADI-PEG20 improved visual contrast sensitivity through 4 weeks in the T2D mouse model. However, the protective effect on visual acuity evident at 2 weeks of treatment was not maintained through 4 weeks. This could be due to limited sample size or development of an immune reaction to ADI. Although pegylation of ADI reduces its immunogenicity, ADI-PEG20 retains enough immunogenicity for development of antibodies against it [18]. This could affect the bio-distribution of ADI-PEG20 due to opsonization and elimination by the reticuloendothelial system [61]. However, this was not seen in the 12-week IM injection study where the improved visual acuity observed with ADI-PEG20 treatment was maintained at 4 weeks and through the remaining time points measured. It is important to note, injections in the12-week were IM while those in the 4 week study were IP. Cancer studies utilizing ADI-PEG20 often administer the drug via IM injections, which was our reasoning for using this route for the 12-week study. Our data suggests IM may be a more effective mode of delivery. Differential distribution of ADI-PEG20 and subsequent development of neutralizing antibodies can be affected by the route of administration, and further studies are needed to optimize treatment outcomes.

In addition to limiting DR in the *db/db* mice, systemic delivery of ADI-PEG20 also protected against diabetes-induced impairment of peripheral sensory function. Obese, diabetic *db/db* mice exhibit impaired peripheral sensory function which can be assessed as delayed paw withdrawal responses to thermal stimuli [45]. We found that ADI-PEG20 maintained thermal sensitivity. Pathological development of diabetic peripheral neuropathy (DPN) in diabetic mice is not well understood [7]. However, there is evidence for involvement of iNOS in DPN in streptozotocin-induced diabetic mice where a reduction in iNOS levels was associated with reduction in DPN [62]. One possibility for the restored thermal sensitivity we observed could be that ADI-PEG20 reduces iNOS expression and levels of NO production via reducing L-arginine availability [50]. Studies on the role of L-arginine depletion in the development of DPN are warranted.

Similar to DPN, cutaneous wound healing is also impaired in *db/db* mice [32]. In our experiments, the IP treatment with ADI-PEG20 significantly improved rate of wound healing. Hyperglycemia is

 

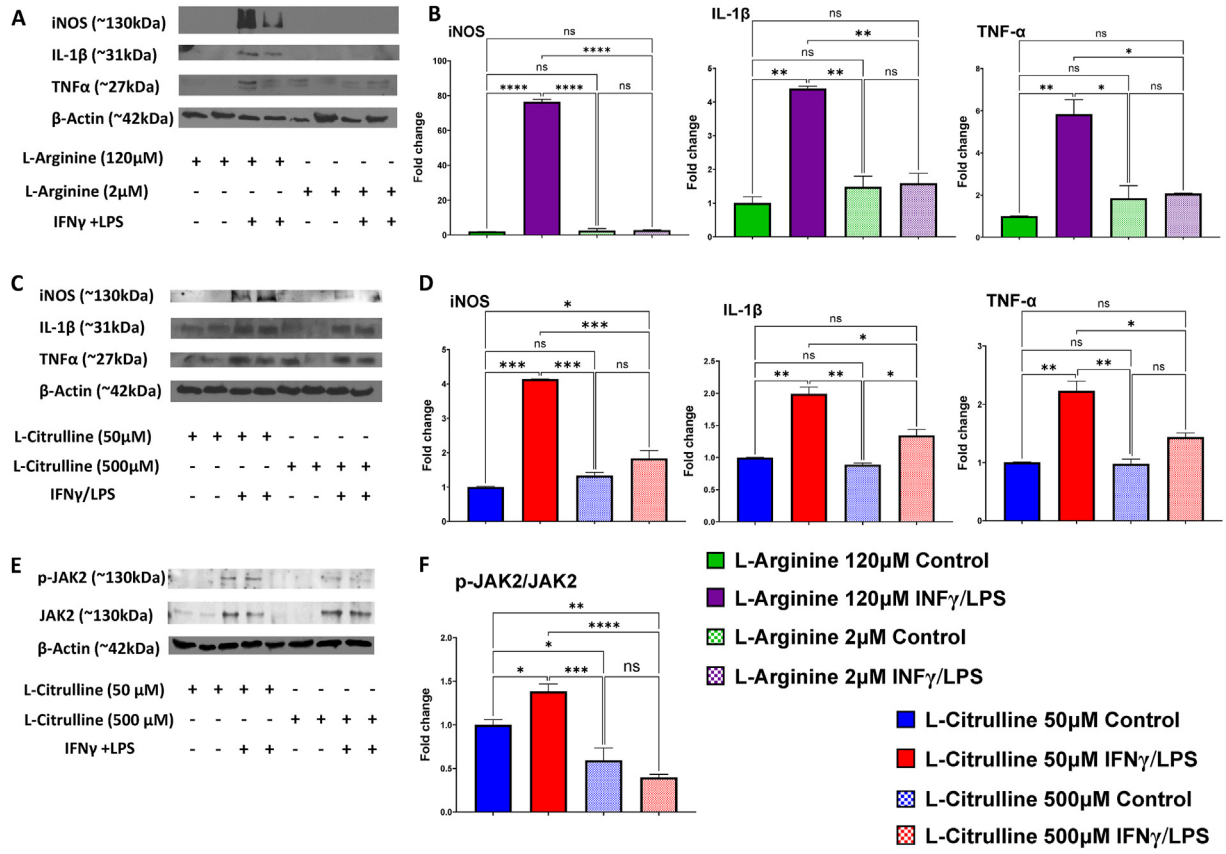


**Figure 8: Effects of L-Arginine and L-Citrulline treatments on markers of inflammation, oxidative stress and JAK/STAT1 signaling in activated BMDM.** Representative western blots and quantitation of iNOS, IL-1β, and TNFα **(A,B,C,D)** in IFNγ/LPS activated BMDM treated with L-Arginine (120 or 2 μM) or L-citrulline (50 or 500 μM). Representative western blots and quantitation of p-JAK2 and JAK2 **(E, F)** in IFNγ/LPS activated BMDM after treatments with 50 or 500 μM of L-Citrulline. ($n = 3$/group). ns = not significant, $^{*}p < 0.05$, $^{**}p < 0.01$, $^{***}p < 0.001$ and $^{****}p < 0.0001$.

known to sensitize macrophage responses to cytokines, and disturb their phagocytic activity [63]. In addition, free fatty acids, such as palmitate, have been reported to increase mTORC1 activation and impair removal of apoptotic cells by macrophages [54]. Together, these effects of the diabetic environment on macrophages result in impaired functions and impaired wound healing [64]. Our *in vitro* studies of LPS-IFNγ-treated BMDM suggest that the anti-inflammatory effects of ADI-PEG20 are likely to involve L-arginine depletion and L-citrulline production. Additional studies of the actions of ADI-PEG20 and elevated levels of L-citrulline on macrophage polarity and reparative functions are strongly warranted.

## 5. CONCLUSION

In conclusion, treatment of obese, diabetic *db/db* mice with ADI-PEG20 limits inflammatory and oxidative damage in the retina, maintains BRB function, and improves visual acuity and contrast sensitivity. This treatment also prevents T2D. Our results support the therapeutic use of ADI-PEG20 in diabetic retinopathy and other diabetic complications. Its safety for human use has been established [18,65].

## 6. LIMITATIONS

While our Western blot analyses showed significant decreases in TNF-α, IL-1β, and iNOS, further studies evaluating additional inflammatory mediators and additional methods (i.e. PCR, ELISA) are needed to fully define the impact of the ADI-PEG20 treatment on the inflammatory responses. Also, the beneficial effects of IVT injections of ADI-PEG20 on BRB and visual function help support an independent effect of the drug treatment on the development of DR. However, because systemic treatment with ADI-PEG20 limits weight gain and hyperglycemia as well as improving DPN and wound healing, we cannot rule out an indirect mechanism in these effects secondary to the suppression of T2D.

## FUNDING

This work was supported by grants from the National Institute of Health (R01-EY11766 to RBC and RWC, R01-EY03568 to MR and RBC, P30 EY031631/EY/NEI NIH to the Culver Vision Discovery Institute at Augusta University), and Polaris Pharmaceuticals, Inc., San Diego, CA.

## CREDIT AUTHORSHIP CONTRIBUTION STATEMENT

**Ammar A. Abdelrahman:** Writing — review & editing, Writing — original draft, Visualization, Validation, Methodology, Investigation, Formal analysis, Conceptualization. **Porsche V. Sandow:** Writing — review & editing, Visualization, Methodology, Investigation, Formal analysis. **Jing Wang:** Writing — review & editing, Writing — original draft, Visualization, Validation, Methodology, Investigation, Formal analysis, Conceptualization. **Zhimin Xu:** Writing — review & editing,

 

Visualization, Validation, Methodology, Investigation, Formal analysis, Data curation. **Modesto Rojas:** Writing — review & editing, Visualization, Methodology, Investigation, Formal analysis. **John S. Bomalaski:** Writing — review & editing, Validation, Resources, Methodology, Funding acquisition, Formal analysis, Conceptualization. **Tahira Lemtalsi:** Writing — review & editing, Visualization, Methodology, Investigation. **Ruth B. Caldwell:** Writing — review & editing, Writing — original draft, Validation, Supervision, Resources, Funding acquisition, Formal analysis, Conceptualization. **Robert W. Caldwell:** Writing — review & editing, Writing — original draft, Validation, Supervision, Resources, Project administration, Funding acquisition, Conceptualization.

## ACKNOWLEDGEMENT

We thank Dr. Syed A. H. Zaidi for his assistance in data analysis and preparation of figures.

## DECLARATION OF COMPETING INTEREST

The authors declare the following financial interests/personal relationships which may be considered as potential competing interests: R. B. Caldwell, M. Rojas, report financial support was provided by National Institutes of Health. Robert W. Caldwell reports a relationship with National Institutes of Health that includes: funding grants. If there are other authors, they declare that they have no known competing financial interests or personal relationships that could have appeared to influence the work reported in this paper.

## DATA AVAILABILITY

Data will be made available on request.

## APPENDIX A. SUPPLEMENTARY DATA

Supplementary data to this article can be found online at https://doi.org/10.1016/j.molmet.2024.102020.

## REFERENCES

[1] WHO. Diabetes. 2021. Available from: https://www.who.int/news-room/fact-sheets/detail/diabetes. [Accessed 31 October 2022].

[2] Hicks CW, Selvin E. Epidemiology of peripheral neuropathy and lower extremity disease in diabetes. Curr Diabetes Rep 2019;19(10):86. https://doi.org/10.1007/s11892-019-1212-8.

[3] Yonekawa Y, Modi YS, Kim LA, Skondra D, Kim JE, Wykoff CC. American society of retina specialists clinical practice guidelines on the management of nonproliferative and proliferative diabetic retinopathy without diabetic macular edema. J Vitreoretin Dis 2020;4(2):125—35. https://doi.org/10.1177/2474126419893829.

[4] Nathan DM. Realising the long-term promise of insulin therapy: the DCCT/EDIC study. Diabetologia 2021;64(5):1049—58. https://doi.org/10.1007/s00125-021-05397-4.

[5] Angermann R, Rauchegger T, Nowosielski Y, Casazza M, Bilgeri A, Ulmer H, et al. Treatment compliance and adherence among patients with diabetic retinopathy and age-related macular degeneration treated by anti-vascular endothelial growth factor under universal health coverage. Graefes Arch Clin Exp Ophthalmol 2019;257(10):2119—25. https://doi.org/10.1007/s00417-019-04414-y.

[6] Gibson DM. Eye care availability and access among individuals with diabetes, diabetic retinopathy, or age-related macular degeneration. JAMA Ophthalmology 2014;132(4):471—7. https://doi.org/10.1001/jamaophthalmol.2013.7682.

[7] Feldman EL, Callaghan BC, Pop-Busui R, Zochodne DW, Wright DE, Bennett DL, et al. Diabetic neuropathy. Nat Rev Dis Prim 2019;5(1):41. https://doi.org/10.1038/s41572-019-0092-1.

[8] Elafros MA, Andersen H, Bennett DL, Savelieff MG, Viswanathan V, Callaghan BC, et al. Towards prevention of diabetic peripheral neuropathy: clinical presentation, pathogenesis, and new treatments. Lancet Neurol 2022;21(10):922—36. https://doi.org/10.1016/S1474-4422(22)00188-0.

[9] Sorber R, Abularrage CJ. Diabetic foot ulcers: epidemiology and the role of multidisciplinary care teams. Semin Vasc Surg 2021;34(1):47—53. https://doi.org/10.1053/j.semvascsurg.2021.02.006.

[10] Rohm TV, Meier DT, Olefsky JM, Donath MY. Inflammation in obesity, diabetes, and related disorders. Immunity 2022;55(1):31—55. https://doi.org/10.1016/j.immuni.2021.12.013.

[11] Fouda AY, Xu Z, Shosha E, Lemtalsi T, Chen J, Toque HA, et al. Arginase 1 promotes retinal neurovascular protection from ischemia through suppression of macrophage inflammatory responses. Cell Death Dis 2018;9(10):1001. https://doi.org/10.1038/s41419-018-1051-6.

[12] Fouda AY, Eldahshan W, Xu Z, Lemtalsi T, Shosha E, Zaidi SAH, et al. Preclinical investigation of Pegylated arginase 1 as a treatment for retina and brain injury. Exp Neurol 2022;348:113923. https://doi.org/10.1016/j.expneurol.2021.113923.

[13] Abdelrahman AA, Bunch KL, Sandow PV, Cheng PN, Caldwell RB, Caldwell RW. Systemic administration of pegylated arginase-1 attenuates the progression of diabetic retinopathy. Cells 2022;11(18). https://doi.org/10.3390/cells11182890.

[14] Caldwell RW, Rodriguez PC, Toque HA, Narayanan SP, Caldwell RB. Arginase: a multifaceted enzyme important in health and disease. Physiol Rev 2018;98(2):641—65. https://doi.org/10.1152/physrev.00037.2016.

[15] Xiong L, Teng JLL, Botelho MG, Lo RC, Lau SKP, Woo PCY. Arginine metabolism in bacterial pathogenesis and cancer therapy. Int J Mol Sci 2016;17(3). https://doi.org/10.3390/ijms17030363.

[16] Feun L, Savaraj N. Pegylated arginine deiminase: a novel anticancer enzyme agent. Expet Opin Invest Drugs 2006;15(7):815—22. https://doi.org/10.1517/13543784.15.7.815.

[17] Butler M, van der Meer LT, van Leeuwen FN. Amino acid depletion therapies: starving cancer cells to death. Trends Endocrinol Metabol 2021;32(6):367—81. https://doi.org/10.1016/j.tem.2021.03.003.

[18] Yao S, Janku F, Koenig K, Tsimberidou AM, Piha-Paul SA, Shi N, et al. Phase 1 trial of ADI-PEG 20 and liposomal doxorubicin in patients with metastatic solid tumors. Cancer Med 2022;11(2):340—7. https://doi.org/10.1002/cam4.4446.

[19] Yao S, Janku F, Subbiah V, Stewart J, Patel SP, Kaseb A, et al. Phase 1 trial of ADI-PEG20 plus cisplatin in patients with pretreated metastatic melanoma or other advanced solid malignancies. Br J Cancer 2021;124(9):1533—9. https://doi.org/10.1038/s41416-020-01230-8.

[20] Han RZ, Xu GC, Dong JJ, Ni Y. Arginine deiminase: recent advances in discovery, crystal structure, and protein engineering for improved properties as an anti-tumor drug. Appl Microbiol Biotechnol 2016;100(11):4747—60. https://doi.org/10.1007/s00253-016-7490-z.

[21] Zhang L, Liu M, Jamil S, Han R, Xu G, Ni Y. PEGylation and pharmacological characterization of a potential anti-tumor drug, an engineered arginine deiminase originated from Pseudomonas plecoglossicida. Cancer Lett 2015;357(1):346—54. https://doi.org/10.1016/j.canlet.2014.11.042.

[22] Holtsberg FW, Ensor CM, Steiner MR, Bomalaski JS, Clark MA. Poly(ethylene glycol) (PEG) conjugated arginine deiminase: effects of PEG formulations on its pharmacological properties. J Contr Release 2002;80(1):259—71. https://doi.org/10.1016/S0168-3659(02)00042-1.

[23] Mohammad MA, Didelija IC, Stoll B, Nguyen TC, Marini JC. Pegylated arginine deiminase depletes plasma arginine but maintains tissue arginine availability

  

in young pigs. Am J Physiol Endocrinol Metabol 2021;320(3):E641–52. https://doi.org/10.1152/ajpendo.00472.2020.

[24] Abou-Alfa GK, Qin S, Ryoo BY, Lu SN, Yen CJ, Feng YH, et al. Phase III randomized study of second line ADI-PEG 20 plus best supportive care versus placebo plus best supportive care in patients with advanced hepatocellular carcinoma. Ann Oncol 2018;29(6):1402–8. https://doi.org/10.1093/annonc/mdy101.

[25] Allerton TD, Proctor DN, Stephens JM, Dugas TR, Spielmann G, Irving BA. L-Citrulline supplementation: impact on cardiometabolic health. Nutrients 2018;10(7). https://doi.org/10.3390/nu10070921.

[26] Ham DJ, Gleeson BG, Chee A, Baum DM, Caldow MK, Lynch GS, et al. L-citrulline protects skeletal muscle cells from cachectic stimuli through an iNOS-dependent mechanism. PLoS One 2015;10(10):e0141572. https://doi.org/10.1371/journal.pone.0141572.

[27] Yuan Y, Mohammad MA, Betancourt A, Didelija IC, Yallampalli C, Marini JC. The citrulline recycling pathway sustains cardiovascular function in arginine-depleted healthy mice, but cannot sustain nitric oxide production during endotoxin challenge. J Nutr 2018;148(6):844–50. https://doi.org/10.1093/jn/nxy065.

[28] Ginguay A, Regazzetti A, Laprevote O, Moinard C, De Bandt JP, Cynober L, et al. Citrulline prevents age-related LTP decline in old rats. Sci Rep 2019;9(1):20138. https://doi.org/10.1038/s41598-019-56598-2.

[29] Szlosarek PW, Creelan BC, Sarkodie T, Nolan L, Taylor P, Olevsky O, et al. Pegargiminase plus first-line chemotherapy in patients with nonepithelioid pleural mesothelioma: the ATOMIC-meso randomized clinical trial. JAMA Oncol 2024;10(4):475–83. https://doi.org/10.1001/jamaoncol.2023.6789.

[30] Yang Q, Xu Y, Xie P, Cheng H, Song Q, Su T, et al. Retinal neurodegeneration in db/db mice at the early period of diabetes. Journal of Ophthalmology 2015;2015:757412. https://doi.org/10.1155/2015/757412.

[31] De Gregorio C, Contador D, Campero M, Ezquer M, Ezquer F. Characterization of diabetic neuropathy progression in a mouse model of type 2 diabetes mellitus. Biol Open 2018;7(9). https://doi.org/10.1242/bio.036830.

[32] Stachura A, Khanna I, Krysiak P, Paskal W, Włodarski P. Wound healing impairment in type 2 diabetes model of leptin-deficient mice-A mechanistic systematic review. Int J Mol Sci 2022;23(15). https://doi.org/10.3390/ijms23158621.

[33] Fouda AY, Xu Z, Suwanpradid J, Rojas M, Shosha E, Lemtalsi T, et al. Targeting proliferative retinopathy: arginase 1 limits vitreoretinal neovascularization and promotes angiogenic repair. Cell Death Dis 2022;13(8):745. https://doi.org/10.1038/s41419-022-05196-8.

[34] Atawia RT, Bunch KL, Fouda AY, Lemtalsi T, Eldahshan W, Xu Z, et al. Role of arginase 2 in murine retinopathy associated with western diet-induced obesity. J Clin Med 2020;9(2):317. https://doi.org/10.3390/jcm9020317.

[35] Douglas RM, Alam NM, Silver BD, McGill TJ, Tschetter WW, Prusky GT. Independent visual threshold measurements in the two eyes of freely moving rats and mice using a virtual-reality optokinetic system. Vis Neurosci 2005;22(5):677–84. https://doi.org/10.1017/S0952523805225166.

[36] Wang J, Saul A, Cui X, Roon P, Smith SB. Absence of Sigma 1 receptor accelerates photoreceptor cell death in a murine model of retinitis pigmentosa. Invest Ophthalmol Vis Sci 2017;58(11):4545–58. https://doi.org/10.1167/iovs.17-21947.

[37] Wu G, Meininger CJ. Analysis of citrulline, arginine, and methylarginines using high-performance liquid chromatography. Methods Enzymol 2008;440:177–89. https://doi.org/10.1016/S0076-6879(07)00810-5.

[38] Benjamini Y, Krieger AM, Yekutieli D. Adaptive linear step-up procedures that control the false discovery rate. Biometrika 2006;93(3):491–507. https://doi.org/10.1093/biomet/93.3.491.

[39] Zhang Y, Higgins CB, Van Tine BA, Bomalaski JS, DeBosch BJ. Pegylated arginine deiminase drives arginine turnover and systemic autophagy to dictate energy metabolism. Cell Rep Med 2022;3(1):100498. https://doi.org/10.1016/j.xcrm.2021.100498.

[40] Kowluru RA. Effect of reinstitution of good glycemic control on retinal oxidative stress and nitrative stress in diabetic rats. Diabetes 2003;52(3):818–23. https://doi.org/10.2337/diabetes.52.3.818.

[41] Antonetti DA, Silva PS, Stitt AW. Current understanding of the molecular and cellular pathology of diabetic retinopathy. Nat Rev Endocrinol 2021;17(4):195–206. https://doi.org/10.1038/s41574-020-00451-4.

[42] Zheng L, Du Y, Miller C, Gubitosi-Klug RA, Kern TS, Ball S, et al. Critical role of inducible nitric oxide synthase in degeneration of retinal capillaries in mice with streptozotocin-induced diabetes. Diabetologia 2007;50(9):1987–96. https://doi.org/10.1007/s00125-007-0734-9.

[43] O'Leary F, Campbell M. The blood–retina barrier in health and disease. FEBS J 2021. https://doi.org/10.1111/febs.16330. n/a(n/a).

[44] Bunch KL, Abdelrahman AA, Caldwell RB, Caldwell RW. Novel therapeutics for diabetic retinopathy and diabetic macular edema: a pathophysiologic perspective. Front Physiol 2022;13:831616. https://doi.org/10.3389/fphys.2022.831616.

[45] Jolivalt CG, Frizzi KE, Guernsey L, Marquez A, Ochoa J, Rodriguez M, et al. Peripheral neuropathy in mouse models of diabetes. Curr Protoc Mol Biol 2016;6(3):223–55. https://doi.org/10.1002/cpmo.11.

[46] Ryan S, Begley M, Gahan CGM, Hill C. Molecular characterization of the arginine deiminase system in Listeria monocytogenes: regulation and role in acid tolerance. Environ Microbiol 2009;11(2):432–45. https://doi.org/10.1111/j.1462-2920.2008.01782.x.

[47] Choi Y, Choi J, Groisman Eduardo A, Kang D-H, Shin D, Ryu S. Expression of stm4467-encoded arginine deiminase controlled by the STM4463 regulator contributes to Salmonella enterica serovar typhimurium virulence. Infect Immun 2012;80(12):4291–7. https://doi.org/10.1128/IAI.00880-12.

[48] Oz HS, Zhong J, de Villiers WJ. Pegylated arginine deiminase downregulates colitis in murine models. Mediat Inflamm 2012;2012:813892. https://doi.org/10.1155/2012/813892.

[49] Izzo F, Montella M, Orlando AP, Nasti G, Beneduce G, Castello G, et al. Pegylated arginine deiminase lowers hepatitis C viral titers and inhibits nitric oxide synthesis. J Gastroenterol Hepatol 2007;22(1):86–91. https://doi.org/10.1111/j.1440-1746.2006.04463.x.

[50] Lee J, Ryu H, Ferrante RJ, Morris Jr SM, Ratan RR. Translational control of inducible nitric oxide synthase expression by arginine can explain the arginine paradox. Proc Natl Acad Sci U S A 2003;100(8):4843–8. https://doi.org/10.1073/pnas.0735876100.

[51] García-Navas R, Munder M, Mollinedo F. Depletion of L-arginine induces autophagy as a cytoprotective response to endoplasmic reticulum stress in human T lymphocytes. Autophagy 2012;8(11):1557–76. https://doi.org/10.4161/auto.21315.

[52] Chantranupong L, Scaria SM, Saxton RA, Gygi MP, Shen K, Wyant GA, et al. The CASTOR proteins are arginine sensors for the mTORC1 pathway. Cell 2016;165(1):153–64. https://doi.org/10.1016/j.cell.2016.02.035.

[53] Zhao Z, Zhang P, Li W, Wang D, Ke C, Liu Y, et al. Pegylated recombinant human arginase 1 induces autophagy and apoptosis via the ROS-activated AKT/mTOR pathway in bladder cancer cells. Oxid Med Cell Longev 2021;2021:5510663. https://doi.org/10.1155/2021/5510663.

[54] Sós L, Garabuczi É, Sághy T, Mocsár G, Szondy Z. Palmitate inhibits mouse macrophage efferocytosis by activating an mTORC1-regulated rho kinase 1 pathway: therapeutic implications for the treatment of obesity. Cells 2022;11(21). https://doi.org/10.3390/cells11213502.

[55] Mao Z, Zhang W. Role of mTOR in glucose and lipid metabolism. Int J Mol Sci 2018;19(7). https://doi.org/10.3390/ijms19072043.

[56] Kaldirim M, Lang A, Pfeiler S, Fiegenbaum P, Kelm M, Bönner F, et al. Modulation of mTOR signaling in cardiovascular disease to target acute and chronic inflammation. Frontiers in Cardiovascular Medicine 2022;9.

[57] Mao Y, Shi D, Li G, Jiang P. Citrulline depletion by ASS1 is required for proinflammatory macrophage activation and immune responses. Mol Cell 2022;82(3):527–541.e527. https://doi.org/10.1016/j.molcel.2021.12.006.

[58] Baydoun AR, Bogle RG, Pearson JD, Mann GE. Discrimination between citrulline and arginine transport in activated murine macrophages: inefficient

 

synthesis of NO from recycling of citrulline to arginine. Br J Pharmacol 1994;112(2):487–92. https://doi.org/10.1111/j.1476-5381.1994.tb13099.x.

[59] Lange SM, McKell MC, Schmidt SM, Hossfeld AP, Chaturvedi V, Kinder JM, et al. l-Citrulline metabolism in mice augments CD4+ T cell proliferation and cytokine production in vitro, and accumulation in the mycobacteria-infected lung. Front Immunol 2017;8.

[60] Romero MJ, Platt DH, Caldwell RB, Caldwell RW. Therapeutic use of citrulline in cardiovascular disease. Cardiovasc Drug Rev 2006;24(3–4):275–90. https://doi.org/10.1111/j.1527-3466.2006.00275.x.

[61] Kolate A, Baradia D, Patil S, Vhora I, Kore G, Misra A. Peg — a versatile conjugating ligand for drugs and drug delivery systems. J Contr Release 2014;192:67–81. https://doi.org/10.1016/j.jconrel.2014.06.046.

[62] Vareniuk I, Pavlov IA, Obrosova IG. Inducible nitric oxide synthase gene deficiency counteracts multiple manifestations of peripheral neuropathy in a streptozotocin-induced mouse model of diabetes. Diabetologia 2008;51(11):2126–33. https://doi.org/10.1007/s00125-008-1136-3.

[63] Pavlou S, Lindsay J, Ingram R, Xu H, Chen M. Sustained high glucose exposure sensitizes macrophage responses to cytokine stimuli but reduces their phagocytic activity. BMC Immunol 2018;19(1):24. https://doi.org/10.1186/s12865-018-0261-0.

[64] Wolf SJ, Melvin WJ, Gallagher K. Macrophage-mediated inflammation in diabetic wound repair. Semin Cell Dev Biol 2021;119:111–8. https://doi.org/10.1016/j.semcdb.2021.06.013.

[65] Szlosarek PW, Steele JP, Nolan L, Gilligan D, Taylor P, Spicer J, et al. Arginine deprivation with pegylated arginine deiminase in patients with argininosuccinate synthetase 1-deficient malignant pleural mesothelioma A randomized clinical trial. JAMA Oncol 2017;3(1):58–66. https://doi.org/10.1001/jamaoncol.2016.3049.

  